This is a repository copy of *Fire behaviour of rectangular steel tubed-reinforced-concrete columns with end restraints*.

White Rose Research Online URL for this paper:
https://eprints.whiterose.ac.uk/id/eprint/218877/

Version: Accepted Version

Article:
Yang, D. orcid.org/0009-0000-0066-9538, Liu, F., Huang, S.-S. orcid.org/0000-0003-2816-7104 et al. (2 more authors) (2024) Fire behaviour of rectangular steel tubed-reinforced-concrete columns with end restraints. International Journal of Steel Structures, 24 (6). pp. 1406-1421. ISSN: 1598-2351

https://doi.org/10.1007/s13296-024-00898-5

This version of the article has been accepted for publication, after peer review (when applicable) and is subject to Springer Nature's AM terms of use, but is not the Version of Record and does not reflect post-acceptance improvements, or any corrections. The Version of Record is available online at: http://dx.doi.org/10.1007/s13296-024-00898-5

Reuse
Items deposited in White Rose Research Online are protected by copyright, with all rights reserved unless indicated otherwise. They may be downloaded and/or printed for private study, or other acts as permitted by national copyright laws. The publisher or other rights holders may allow further reproduction and re-use of the full text version. This is indicated by the licence information on the White Rose Research Online record for the item.

Takedown
If you consider content in White Rose Research Online to be in breach of UK law, please notify us by emailing eprints@whiterose.ac.uk including the URL of the record and the reason for the withdrawal request.

eprints@whiterose.ac.uk
https://eprints.whiterose.ac.uk/

Dongdong Yang*, Faqi Liu, Shan-Shan Huang, Hua Yang, Kun Wang. Fire behaviour of rectangular steel tubed-reinforced-concrete columns with end restraints, International Journal of Steel Structures, 2024. DOI: 10.1007/s13296-024-00898-5

Fire behaviour of rectangular steel tubed-reinforced-concrete columns with end restraints

Dongdong Yang[1,2,*], Faqi Liu[3,4], Shan-Shan Huang[5], Hua Yang[3,4], and Kun Wang[2]

[1] Zhejiang Engineering Research Center of Intelligent Urban Infrastructure, Hangzhou City University, 310015

[2] Department of Civil Engineering, College of Architectural Science and Engineering, Yangzhou University, Yangzhou, 225127, China

[3] Key Lab of Structures Dynamic Behaviour and Control (Harbin Institute of Technology), Ministry of Education, Heilongjiang, Harbin 150090, China

[4] Key Lab of Smart Prevention and Mitigation of Civil Engineering Disasters (Harbin Institute of Technology), Ministry of Industry and Information Technology, Heilongjiang, Harbin 150090, China

[5] Department of Civil and Structural Engineering, The University of Sheffield, Sheffield S1 3JD, UK

Abstract

The steel tubed-reinforced-concrete (STRC) column is a new form of composite column, in which the steel tube primarily serves to provide confinement to concrete core rather than directly carrying axial force. The restraining effects at the heated column ends should be incorporated into the fire performance design of STRC columns, while current research on rectangular STRC columns is still inadequate. This study presents the numerical study on the fire behaviour of end-restrained rectangular STRC columns. The effects of axial restraint and rotational restraint on the overall deformations, internal forces, fire resistance, axial force and buckling length at fire limit state, of rectangular STRC columns with various cross-sectional sizes, aspect ratios, slenderness ratios and load ratios were thoroughly analyzed. The end-restrained rectangular STRC columns fail in fire mainly due to runaway of axial contraction, and the failure mode may shift from dynamic to static as the axial restraint increases. The fire resistance of rectangular STRC columns subjected to bending around the major axis is generally higher than in the case of minor-axis bending. The axial force inside the column decreases nearly linearly while the fire resistance experiences an almost linear increase with increasing the axial restraint ratio. The beneficial effect of rotational restraint, i.e. decreasing the buckling length and enhancing the fire resistance is prominent, especially for columns under relatively low restraining levels. Finally, simplified equations were given for designing the structural fire performance of rectangular STRC columns with considering the end restraining effects.

Keywords

Rectangular steel tubed-reinforced-concrete columns, Fire performance, End restraints, Finite element analysis, Buckling length

1 Introduction

The steel tubed-reinforced-concrete (STRC) is a new steel-concrete composite column form that comprises an outer steel tube and an inner reinforced concrete (RC) section (Zhou et al., 2023). The steel tube in a STRC column is discontinuous at the joint zone (as shown in Fig. 1), thus it is designed not to carry load axially but to provide sufficient lateral confinement to the concrete. Consequently, the axial load applied onto a STRC mainly acts on the confined RC part. This is significantly different from traditional concrete-filled steel tubular (CFST) columns that may or may not contain internal steel reinforcements; in such cases, the steel tube sustains the axial load together with the inner plain concrete or RC section. The steel tube in a STRC column could confine the concrete core more effectively, and its local buckling is effectively minimized. Owing to the excellent load-bearing capacity, good seismic performance, and construction convenience, STRC columns are increasingly being utilized in engineering (Zhou & Liu, 2019). Fig. 1 shows a representative application of STRC columns used in a super high-rise building in China, namely the Qingdao Haitian Tower 3 (245 m in height).

Fire performance is a crucial design consideration for STRC columns, as their steel tubes may be directly exposed to fire. To date, extensive experimental and numerical studies have been reported on the fire performance, as well as the post-fire performance, of pin-ended STRC columns with circular, square, and rectangular sections (Liu et al., 2014; Liu et al., 2019a; Liu et al., 2019b; Yang et al., 2020; Zhang et al., 2020; Zhou et al., 2021; Yang et al., 2021a). STRC columns have been observed to exhibit excellent performance under fire

conditions. Comprehensive methods for designing the fire resistance and determining the necessary fireproof thickness of STRC columns have been developed.

In real structures, the heated STRC columns are restrained by the adjacent beams and columns. The restraints at the ends of columns in non-sway plane frames are generally categorized into axial and rotational components. The fire performance of square STRC columns with end restraints has been numerically investigated (Yang et al., 2021b). It is concluded that STRC columns with end restraints exhibit distinct behaviour compared to columns without restraints, since end restraints largely affect the internal force redistribution and buckling length of the column. Till now, no research is available concerning the fire behaviour of rectangular STRC columns with considering the end restraining effects. Compared to square STRC columns, the working mechanics of fire-exposed rectangular STRC columns is more complex, due to the highly non-uninform distribution of confinement effect. Furthermore, the influences of axial and rotational end restraints on the fire behaviour of rectangular STRC columns may also be related to the variation of bending axis.

Based on the previous work (Yang et al., 2021b), this study aims to numerically investigate the fire behaviour of end-restrained rectangular STRC columns via finite element analysis (FEA). The influences of axial restraint and rotational restraint on the evolution of deformations and internal forces during heating as well as on the axial force, buckling length and fire resistance, of rectangular STRC columns with varying cross-sectional sizes, aspect ratios, slenderness ratios and load ratios were systematically analyzed through parametric studies. Finally, practical formulae were recommended for the structural fire design of rectangular STRC columns, taking into account the effects of end restraints. This study is

expected to serve as a basis and contribute valuable insights for the fire performance research and design considerations of STRC columns within real framed structures, offering a reference framework for future engineering applications.

2 FEA modelling

2.1 Model setup

The sequentially-coupled thermo-mechanical FEA models using ABAQUS were developed to simulate the behaviour of fire-exposed rectangular STRC columns with end restraints. Considering the symmetries of loading conditions and geometric dimensions, only half of the column section was modelled, as shown in Fig. 2. The axial and rotational restraints were modelled using the Spring 1 elements in ABAQUS. Each spring was connected to the reference point at one end, and the other end was fixed. Rotational springs were assigned at the two ends of the column, while the axial spring was located only at one end of the column.

In engineering practice, a heated STRC column is typically subjected to the combined effects of axial and unequal rotational restraints at its upper and lower ends. Furthermore, the restraints at the column ends may vary with temperature due to the direct or indirect fire exposure of the surrounding members. This paper, as an initial study, primarily focuses on columns with constant end restraints. The axial and rotational restraints were investigated separately and the upper and lower rotational restraints were assumed to be equal in this research. The effects of end restraint were only taken into consideration in the mechanical analysis as it did not affect the heat transfer results.

Two normalized ratios α and β were used to quantify the axial and rotational restraining

effects at column ends, as expressed in Eq. (1) and Eq. (2), respectively. α (or β) was defined as the ratio between the axial (or rotational) restraint stiffness k_a (or k_r), provided by adjacent columns and beams at room temperature, to the ambient-temperature compression (or flexural) stiffness k_{ac} (or k_{rc}) of the heated STRC column. In accordance with the previous recommendation (Yang et al., 2021b), the investigated scope of α was 0 to 0.1, and β was set between 0 to 0.5.

$$\alpha = k_a / k_{ac} \tag{1}$$

$$\beta = k_r / k_{rc} \tag{2}$$

where k_{ac} (= $(E_cA_c+E_bA_b)/L$) is the ambient-temperature axial stiffness of the STRC column; k_{rc} (= $4(E_cI_c+E_bI_b+E_sI_s)/L$) is the ambient-temperature rotational stiffness of the STRC column; E_c, E_b and E_s are the elastic moduli of the concrete, rebar and steel tube, respectively; A_c and A_b are the cross-sectional areas of the concrete and rebars, respectively; I_c, I_b and I_s are the second moments of area of the concrete, rebars and steel tube with respect to the centroidal axis of the composite section, respectively; L is the column height.

To enable comparison, rectangular STRC columns with different aspect ratios k_i (the ratio between the height H_i and width B_i of the section), but with the same cross-sectional area and steel ratio, together with an equivalent square column with width D_{eq} ($H_i \cdot B_i = D_{eq}^2$) were investigated. Values of 1.2, 1.5, 1.8 and 2.0 were used for k_i, following the maximum aspect ratio regulations for rectangular CFST columns given in the Chinese design specification CECS 159 (2004). As presented in Fig. 3, the rectangular STRC columns were labelled as Rk_i-Maj and Rk_i-Min, based on their respective bending axes. While varying the aspect ratios and bending axes, the slenderness ratio of the columns remained constant. The default values

of other parameters were: concrete cube compressive strength of 50 MPa, steel tube yield strength of 355 MPa, yield strength of reinforcing bar of 335 MPa, steel tube ratio of 3%, reinforcement ratio of 4%, and a concrete cover of 25 mm for the reinforcement. Given that the fire behaviour of restrained STRC columns is mainly affected by the end restraint levels (Yang et al., 2021b), fixed steel tube ratio and reinforcement ratio were adopted in this study. The values of these two parameters were selected following the regulations specified in the Chinese design standard JGJ/T471 (2020). Considering the negligible influence of stirrups on the fire resistance of STRC columns, as concluded in prior research (Yang et al., 2020; Yang et al., 2021a), only longitudinal reinforcements were incorporated in the FEA model. The arrangement, sizes and spacing of reinforcing bars for each cross-section, were determined according to the dimension of the composite section, the reinforcement ratio, the steel tube thickness and the concrete cover. The parameters of the FEA models constructed and analyzed in the presented numerical investigation are summarized in Table 1.

All the columns were uniformly heated along their entire heights, following the ISO 834 standard fire regime. Other details of the FEA models, e.g. the material properties, interaction and constraint, element types and meshing, were the same as those used in the previous study (Yang et al., 2021b) and were not repeated here. Currently, there are no specific definitions related to the fire resistance of end-restrained composite columns. To remain consistent with the previous work (Yang et al., 2021b), the criteria for unrestrained column specified in ISO 834 (1999) are used. The fire limit state of a restrained column is reached when the axial deformation exceeds $L/100$ or when the deformation rate reaches $3L/1000$ mm/min (L is in mm).

2.2 Model validation

The authors have performed extensive FEA on the fire performance of 11 STRC columns and 23 CFST columns with pin-ended conditions (Yang et al., 2020; Yang et al., 2021a), utilizing the models developed in Section 2.1. Owing to the fact that there are currently no fire tests available for end-restrained STRC columns, the FEA models were validated against the test data of 34 CFST columns with axial and rotational restraints (Pires et al., 2012; Rodrigues & Laim., 2017a; Rodrigues & Laim., 2017b). Detailed comparison results between the modelled and measured data of the developments of temperature, axial deformation and restraining force, have been reported by the authors (Yang et al., 2021b).

Fig. 4 shows the summarization of the ratios between the FEA-modelled critical time $t_{cr,F}$, the axial force ratio $(P_{max}/P_0)_F$ (P_{max} is the maximum force in the column during heating and P_0 is the initial axial load) and the corresponding experimental data $t_{cr,t}$ and $(P_{max}/P_0)_t$. The ratios $t_{cr,F}/t_{cr,t}$ and $(P_{max}/P_0)_F/(P_{max}/P_0)_t$ generally fall within the range of $\pm$20% and achieve mean values of 1.09 and 1.06, respectively. The discrepancies between the FEA and measured data may be attributed to the complexity of fire tests, as well as variations in end restraint stiffness and material properties utilized in the FEA simulations compared to the actual tests. Given the high variability of fire resistance tests, the FEA model is deemed adequate in simulating the performance of end-restrained composite columns. Therefore, it is confidently employed in the subsequent analysis.

3 Effects of axial restraints

3.1 Discussions of results

The influences of axial restraints on the fire behaviour of rectangular STRC columns are first assessed. It should be noted that when the restraint ratio remains constant, the applied axial stiffness differs for rectangular STRC columns with various aspect ratios and bending axes. This arises from the fact that columns with identical cross-sectional areas but different aspect ratios possess distinct axial stiffness characteristics.

Fig. 5 gives typical axial deformation vs. heating time curves for rectangular STRC columns with an equivalent cross-section width D_{eq} of 600 mm, a slenderness ratio λ of 30 and a load ratio n of 0.5. The axial load ratio of a STRC columns is defined as the ratio between the constant load initially applied onto the column before heating and the column's ambient-temperature buckling capacity that determined following the method given in JGJ/T471 (2020). Regardless of the bending axis, both the axial deformation and its rate decrease as the axial restraint ratio increases for columns with aspect ratios of 1.2 and 1.8. This aligns with the findings observed in end-restrained square STRC columns (Yang et al., 2021b). As expected, the rectangular STRC column subjected to bending around the major axis exhibits a greater axial deformation compared to the case of minor-axis bending.

Most of the axially-restrained columns investigated in this study experience the failure caused by the runaway of axial deformation, a dynamic mode. However, for slender rectangular STRC columns with relatively large axial restraint stiffness (e.g. α=0.1 in Fig. 6 for the R1.8-Min column with D_{eq}=600 mm, λ=50, n=0.5), the failure mode may be transferred from dynamic to

static, indicating the progressive collapse of the whole structures in fire could be effectively minimized (Jiang & Li., 2017).

As shown in Fig. 5, the rectangular STRC columns examined in this research experience predominantly axial contraction during heating. A portion of the applied axial load is transferred to the spring, resulting in a reduction of the axial force within the column. In this study, the concept of axial force ratio is introduced, which refers to the ratio between the time-varying axial force within the column and its buckling resistance at ambient temperature. Fig. 7 presents the relationships between the FEA-outputted axial force ratio and heating time for the representative columns illustrated in Fig. 5. As the level of axial restraint increases, the axial force ratio decreases, and the descending rate of axial force increases simultaneously. This indicates a substantial improvement in the positive influence of axial restraint on the fire performance of the column. It is also noted that the vibration of the bending axis has a minimal effect on the axial force ratio of the column. This is primarily because the load ratio and axial restraint ratio remain constant for columns with varying bending axes.

The influences of axial restraint ratios on the fire resistance of rectangular STRC columns with different aspect ratios (1.2 to 1.8), bending axes (major- and minor-), equivalent widths (400 to 1500 mm), slenderness ratios (30 and 50) and load ratios (0.3 to 0.7) are presented in Fig. 8. The increase in axial restraint ratio leads to an almost linear increase in fire resistance. In general, when subjected to major-axis bending, the rectangular STRC column tends to exhibit higher fire resistance compared to a minor-axis bending counterpart.

The axial force ratio of the column at the fire limit state is named as limit axial force ratio n_f. The calculation results of n_f for columns with various parameters are extracted from FEA and

depicted in Fig. 9. Similar to the observation in end-restrained square STRC columns (Yang et al., 2021b), the limit axial force ratios of axially-restrained rectangular STRC columns also exhibit a near-linear decrease as axial restraint stiffness increases. Both the sectional aspect ratio and bending axis hardly affect the limit axial force ratio of the columns.

3.2 Design methods

Different from pin-ended columns, rectangular STRC columns with axial restraints fail in fire when the high-temperature buckling resistance $N_{b,T}$ decreases to the axial force inside the column during heating, as illustrated in Fig. 10. This explains why the fire resistance $t_{FR,a}$ of axially-restrained STRC columns is extended compared to that $t_{FR,p}$ of the unrestrained column. It is crucial to consider the influences of axial restraints when designing the fire safety of rectangular STRC columns in frame structures. The corresponding failure criterion of axially-restrained rectangular STRC columns is expressed as Eq. (3), in which $N_{b,T}$ represents the buckling resistance at elevated temperatures that is given by Eq. (4).

$$N_{b,T} / N_{b} \geq n_{f} \tag{3}$$

$$N_{b,T} = \varphi_{T} N_{u,T} \tag{4}$$

where N_{b} and $N_{u,T}$ are the buckling resistance at ambient temperature and compressive resistance in fire condition, respectively, which could be calculated using the previously-proposed equations (Yang et al., 2021a); φ_T is the high-temperature buckling reduction coefficient, which is recommended to be determined using the buckling curve (c) specified in EC3 (2005) or the square buckling curve given in JGJ/T471 (2020).

To quantitatively address the axial restraining effect on the fire performance of STRC

columns, the authors have recommended a practical equation for determining the limit axial force ratio n_f of square STRC columns with axial restraints (Yang et al., 2021b), as shown in Eq. (5).

$$n_f = n - \left(3.6 - 0.047\lambda\right)\alpha \quad (5)$$

Fig. 11(a) compares the formula-calculated limit axial force ratio using Eq. (5) and the FEA results. The average ratio between the calculated and FEA-extracted axial force ratio is 1.01, with a standard deviation of 0.03. The buckling resistance $N_{b,T}$ of rectangular STRC columns with axial restraints is determined using Eq. (4) and compared with the limit axial force obtained from FEA modelling, and the results are shown in Fig. 11(b). When using the buckling curve (c) in EC3, the average ratio between the buckling resistance and the limit axial force is 0.97, with a standard deviation of 0.08. The comparison shown in Fig. 11 demonstrates that 1) Eq (5), which was originally proposed for square STRC columns, could be applied to rectangular STRC columns for calculating the limit axial force ratio; 2) the fire resistance of axially-restrained rectangular STRC columns could be determined by combining Eqs. (3), (4) and (5).

4 Effects of rotational restraints

4.1 Discussions of results

The main parameters investigated in this section are D_{eq} (400 to 1500 mm), λ (30 and 50) and n (0.5 to 0.7). The influences of rotational restraints on the fire resistance of rectangular STRC columns are depicted in Fig. 12. As expected, the presence of rotational restraint could effectively enhance the fire resistance of the column. In particular, the positive impact of

rotational restraint is particularly noticeable when the restraint ratio is relatively low (e.g. lower than 0.1). These findings align with previous research conducted on rotationally-restrained square STRC columns (Yang et al., 2021b). Rectangular STRC columns with bending around the major axis typically exhibit larger fire resistance compared to columns with bending along the minor axis.

As the heating time increases, the buckling length of a heated STRC column gradually decreases. This is due to the reduction in the flexural stiffness of the heated column, which results in an increased level of relative restraint exerted on the column (Yang et al., 2021b). In fire-resistant design, it is essential to determine the high-temperature buckling length L_{eff} of the column at failure state, i.e. the distance between two bending moment zero points. These points are determined through the FEA-modelled distributions of bending moment along the column height, as shown by typical examples in Fig. 13. The mid-span bending moment of the column gradually decreases as the rotational restraint increases. The rectangular STRC column with major-axis bending experiences a larger bending moment compared to the minor-axis bending case, which is primarily due to the difference in flexural stiffness between two axes.

Fig. 14 presents the buckling length ratio μ_{f} at failure of rectangular STRC columns with various rotational restraint ratios. The existence of rotational restraint could effectively decrease the buckling length of the column. In particular, as β increases from 0 to 0.5, the buckling length ratio decreases from 1.0 to around 0.5, implying the boundary condition of the column is changing from pin-ended to almost fixed. Generally, the influences of bending axis and aspect ratio on the failure buckling length ratio of the columns are marginal.

4.2 Design methods

The rotationally-restrained STRC columns reach the limit state when the buckling resistance $N_{b,T}$ decreases to the initially-applied axial load. However, the high-temperature buckling resistance of a STRC column with rotational restraint decreases at a slower rate than that of an unrestrained column. Therefore, the fire resistance $t_{FR,r}$ of the restrained column becomes longer, as demonstrated in Fig. 15. Eq. (4) is applicable to rectangular STRC columns with rotational restraints, provided that the buckling length ratio is taken into account when calculating φ_T.

The authors have developed a practical equation Eq. (6) to calculate μ_f of square STRC columns with rotational restraints (Yang et al., 2021b).

$$\mu_f = \frac{1+0.41\beta_t}{1+0.82\beta_t} \tag{6}$$

where $\beta_t = \left(60a_{n,D}t+1\right)\beta$; $a_{n,D} = 0.094/D + n - 0.46$ and D (in m) is the width of the square section.

The applicability of Eq. (6) to rectangular STRC columns with rotational restraints is evaluated by replacing the cross-sectional width D in the original formula with the equivalent width D_{eq} ($D_{eq} = \sqrt{HB}$). Fig. 16(a) compares the calculated μ_f and the modelling results that determined using the zero-bending moment method, achieving an average ratio of 1.02 and a standard deviation of 0.05.

With Eq. (6), the buckling resistance of rectangular STRC columns with rotational restraints could be calculated using Eq. (4). The buckling reduction coefficient φ_T is determined in accordance with the EC3 buckling curve (c). As shown in Fig. 16(b), Eq. (4) and Eq. (6) give

an accurate prediction of the buckling resistance of rotationally-restrained rectangular STRC columns in fire, achieving a mean value of 0.96 and a standard deviation of 0.08. This demonstrates that the failure buckling length ratio calculation equation Eq. (6) that previously developed for square STRC columns could be applied to the fire performance design of rectangular STRC columns with rotational restraints, just by using the equivalent cross-sectional width.

5 Conclusions

This study presents numerical investigations to understand the behaviour of end-restrained rectangular STRC columns in fire conditions. The effects of end restraints on the axial deformation, axial force, buckling length, as well as fire resistance of the columns, are obtained via FEA modeling. The following conclusions are drawn:

1) As the axial restraining effect increases, the failure mode of rectangular STRC columns transitions from a dynamic mode to a static mode. Both axially- and rotationally-restrained rectangular STRC columns exhibit better fire performance than unrestrained columns.

2) With an increasing axial restraint, the column demonstrates an almost linear increase in fire resistance, while the limit axial force decreases approximately linearly. As the rotational restraint increases, the buckling length ratio of the column at the failure state decreases from 1 to 0.5, and the fire resistance is significantly prolonged, which is particularly prominent when the restraint ratio is no larger than 0.1.

3) Rectangular STRC columns that experience major-axis bending generally exhibit higher fire resistance than columns subjected to bending around the minor axis. The influences of aspect ratio and bending axis on the axial force ratio and buckling length ratio at the failure state of end-restrained rectangular STRC columns are negligible.

4) The equations given for the limit axial force ratio and failure buckling length ratio, along with the previous methods for unrestrained columns (Yang et al., 2021a), provide an approach for designing the fire performance of rectangular STRC columns with either axial or rotational restraints.

This study serves as a valuable reference for the performance-based fire safety design of STRC structures. Ongoing research is being carried out to further explore the fire behaviour of end-restrained rectangular STRC columns. This includes considering unequal rotational restraints at two ends, combining axial and rotational restraints, and incorporating time-varying restraining effects.

Acknowledgements

The authors gratefully acknowledge the National Natural Science Foundation of China (52308534), the Natural Science Foundation of the Jiangsu Province of China (BK20220592), the Zhejiang Engineering Research Center of Intelligent Urban Infrastructure (IUI2023-YB-10) and the Open Project Program of Guangdong Provincial Key Laboratory of Intelligent Disaster Prevention and Emergency Technologies for Urban Lifeline Engineering (2022ZB05), for the financial support.

References

Zhou, X. H., Liu, J. P., Wang, X. D. (2023). Steel Tube Confined Concrete Structures. Beijing: Science Press, pp. 2–4. (in Chinese)

Zhou, X. H., Liu, J. P. (2019). Application of steel-tubed concrete structures in high-rise buildings. International Journal of High-Rise Buildings, 8(3): 161–167.

Liu, F. Q., Gardner, L., Yang, H. (2014). Post-fire behaviour of reinforced concrete stub columns confined by circular steel tube. Journal of Constructional Steel Research, 102,

82–103.

Liu, F. Q., Wang, Y. Y., Gardner, L., Varma, A. (2019a). Experimental and numerical studies of reinforced concrete columns confined by circular steel tubes exposed to fire. Journal of Structural Engineering, 145(11), 04019130.

Liu, F. Q., Yang, H., Yan, R., Wang, W. (2019b). Experimental and numerical study on behaviour of square steel tube confined reinforced concrete stub columns after fire exposure. Thin-Walled Structures, 139, 105–125.

Yang, D. D., Liu, F. Q., Huang, S., Yang, H. (2020). ISO 834 standard fire test and mechanism analysis of square tubed-reinforced-concrete columns. Journal of Constructional Steel Research, 175, 106316.

Zhang, R. Z., Liu, J. P., Wang, W. Y., Chen, Y. F. (2020). Fire behaviour of thin-walled steel tube confined reinforced concrete stub columns under axial compression. Journal of Constructional Steel Research, 172: 106180.

Zhou, X. H., Yang, J. J., Liu, J. P., Wang, S., Wang, W. Y. (2021). Fire resistance of thin-walled steel tube confined reinforced concrete middle-length columns: test, simulation and design method. Structures, 34: 339–355.

Yang, D. D., Liu, F. Q., Huang, S., Yang, H. (2021a). Structural fire safety design of square and rectangular tubed-reinforced-concrete columns. Structures, 29, 1286–1321.

Yang, D. D., Liu, F. Q., Huang, S., Yang, H. (2021b). Structural behaviour and design of end-restrained square tubed-reinforced-concrete columns exposed to fire. Journal of Constructional Steel Research, 182, 106675.

CECS 159 (2004). Technical Specification for Structures with Concrete-filled Rectangular

Steel Tube Members, CECS (China Association for Engineering Construction Standardization), Beijing, China. (In Chinese)

JGJ/T471 (2020). Technical Standard for Steel Tube Confined Concrete Structures, MOHURD (Ministry of Housing and Urban-Rural Development of the People's Republic of China), Beijing, China. (In Chinese)

ISO 834-1 (1999). Fire Resistance Test - Elements of Building Construction, Part 1: General Requirements, International Organization for Standardization ISO 834, Geneva, Switzerland.

Pires, T. A. C., Rodrigues, J. P. C., Silva. J. J. R. (2012). Fire resistance of concrete filled circular hollow columns with restrained thermal elongation. Journal of Constructional Steel Research, 77(10), 82–94.

Rodrigues, J. P. C., Laím, L. (2017a). Fire resistance of restrained composite columns made of concrete filled hollow sections. Journal of Constructional Steel Research, 133, 65–76.

Rodrigues, J. P. C., Laím, L. (2017b). Fire response of restrained composite columns made with concrete filled hollow sections under different end-support conditions. Engineering Structures, 141, 83–96.

Jiang, J., Li, G. Q. (2017). Progressive collapse analysis of 3D steel frames with concrete slabs exposed to localized fire. Engineering Structures, 149, 21–34.

EN 1993-1-1 (2005). Eurocode 3 - Design of Steel Structures - Part 1-1: General Rules and Rules for Buildings, CEN, Brussels.

Tables

Table 1

Parameters of the FEA models constructed and analyzed in this study

Parameters	Values
Axial restraint ratio α	0, 0.01, 0.03, 0.05, 0.1
Rotational restraint ratio β	0, 0.005, 0.01, 0.02, 0.03, 0.05, 0.1, 0.3, 0.5
Aspect ratio k	1.0, 1.2, 1.5, 1.8, 2.0
Equivalent width D_{eq} (mm)	400, 600, 1000, 1500
Load ratio n	0.3, 0.5, 0.6, 0.7
Slenderness ratio λ	30, 50
Cube compressive strength of concrete f_{cu} (MPa)	50
Yield strength of steel tube f_y (MPa)	355
Yield strength of reinforcing bar f_b (MPa)	335
Steel tube ratio α_s	3%
Reinforcement ratio ρ	4%

Figures

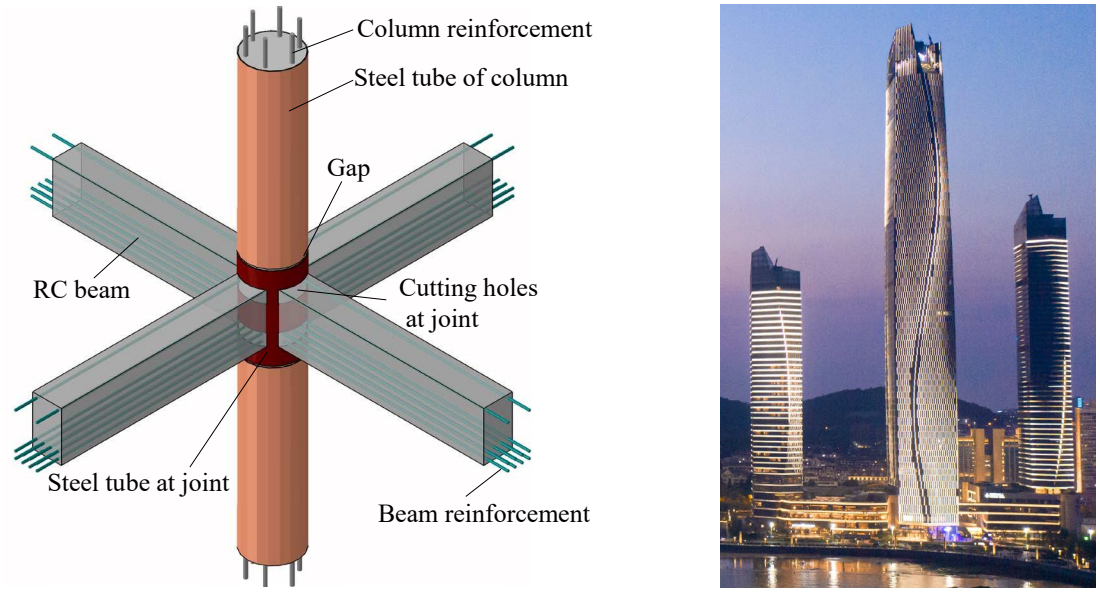

Fig. 1 Typical configuration and engineering application of STRC columns

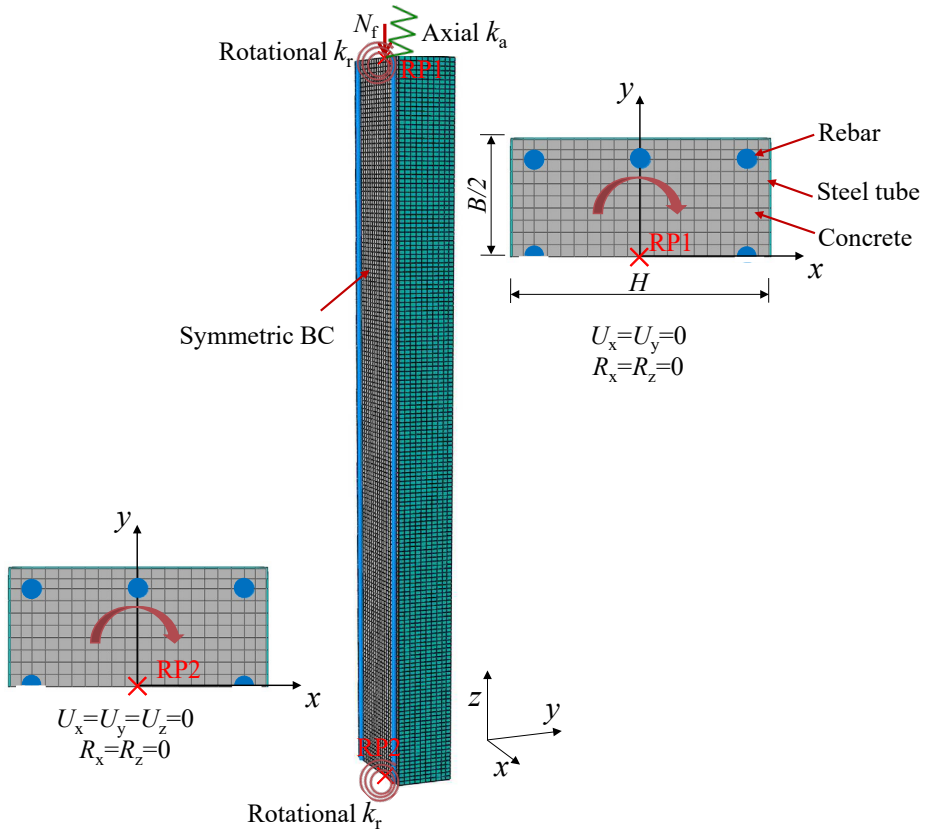

Fig. 2 Finite element modelling of rectangular STRC columns with end restraints (major-axis bending)

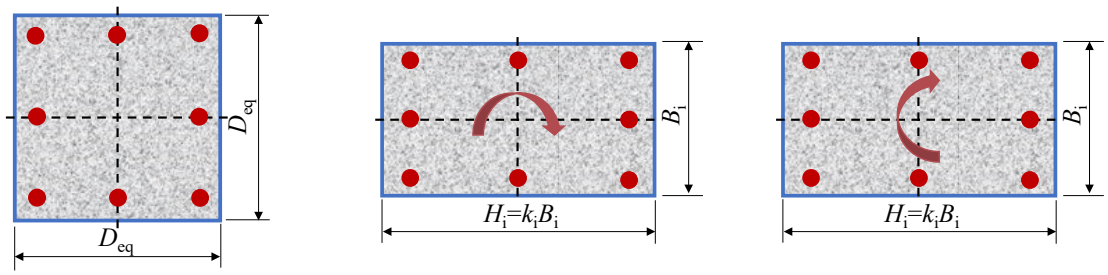

(a) Square (b) Rk_i-Maj (c) Rk_i-Min

Fig. 3 Illustration and naming of rectangular STRC sections

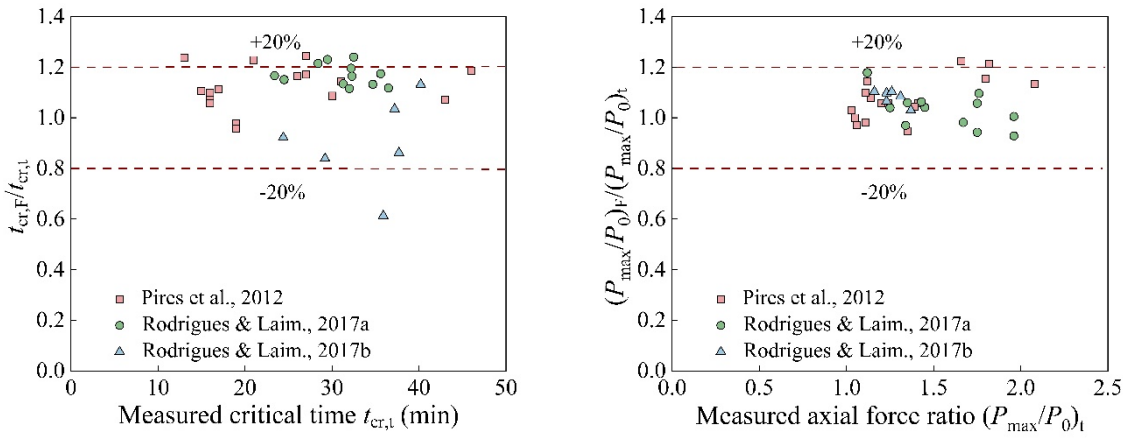

(a) Critical time (b) Axial force ratio

Fig. 4 Validation of the FEA model using the test data of end-restrained CFST columns

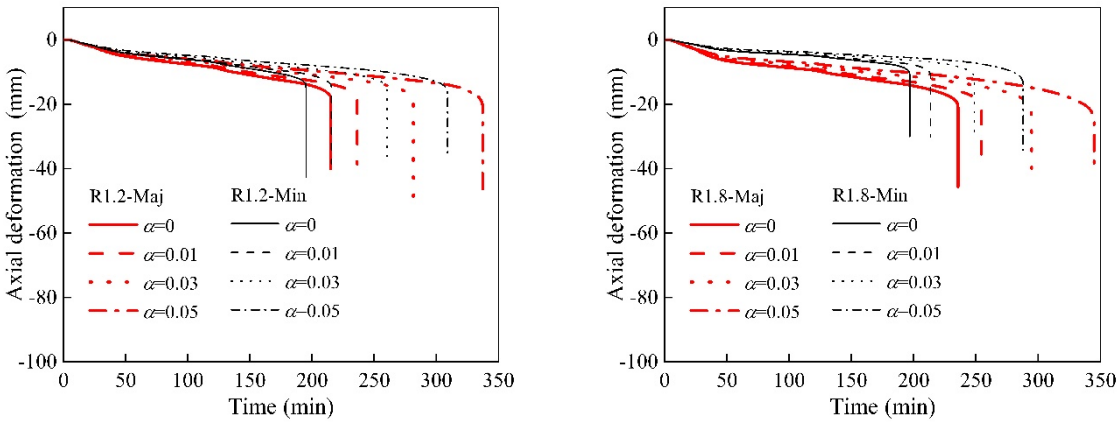

(a) R1.2 columns (b) R1.8 columns

Fig. 5 Axial deformation-time curves of rectangular STRC columns with various axial restraint ratios (D_{eq}=600 mm, n=0.5, λ=30)

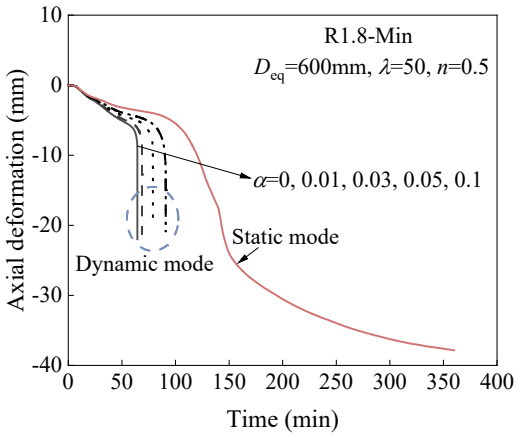

Fig. 6 Transition of failure modes for rectangular STRC columns with various axial restraint ratios (D_{eq}=600 mm, n=0.5, λ=50)

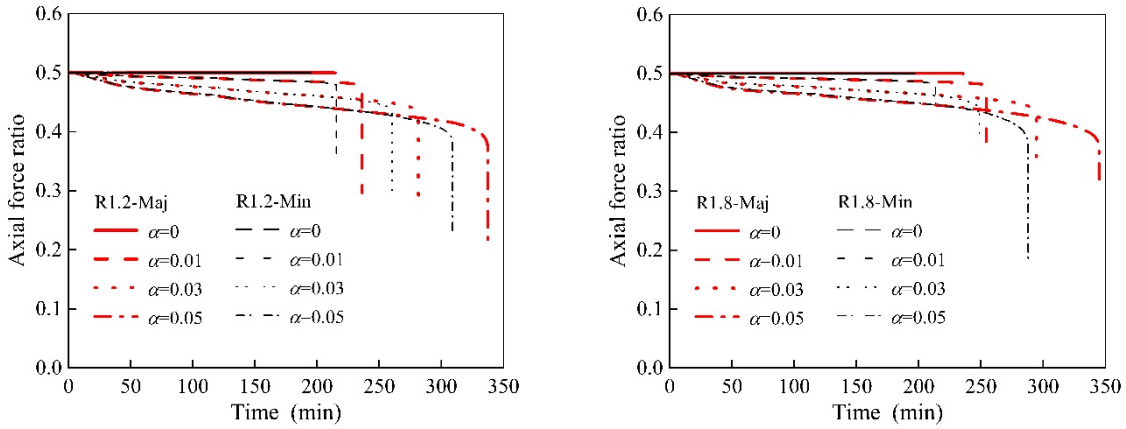

(a) R1.2 columns (b) R1.8 columns

Fig. 7 Axial force ratio-time curves of rectangular STRC columns with various axial restraint ratios (D_{eq}=600 mm, n=0.5, λ=30)

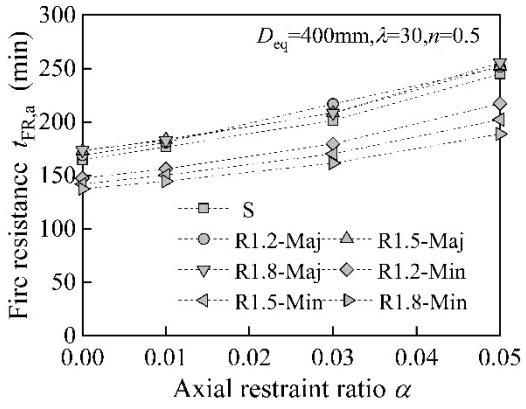

(a) D_{eq}=400mm, n=0.5, λ=30

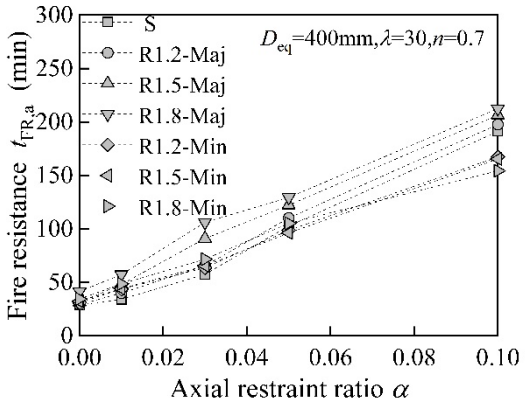

(b) D_{eq}=400mm, n=0.7, λ=30

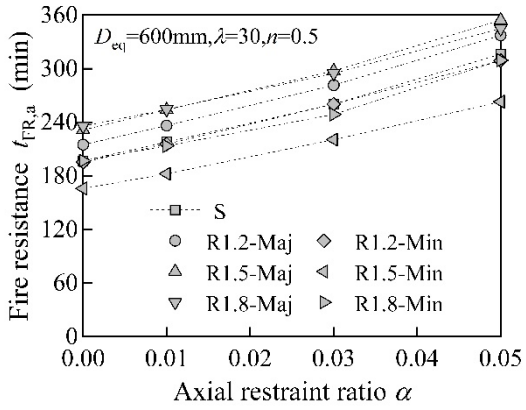

(c) D_{eq}=600mm, n=0.5, λ=30

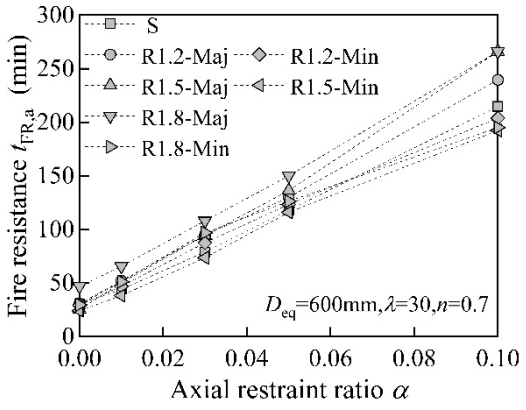

(d) D_{eq}=600mm, n=0.7, λ=30

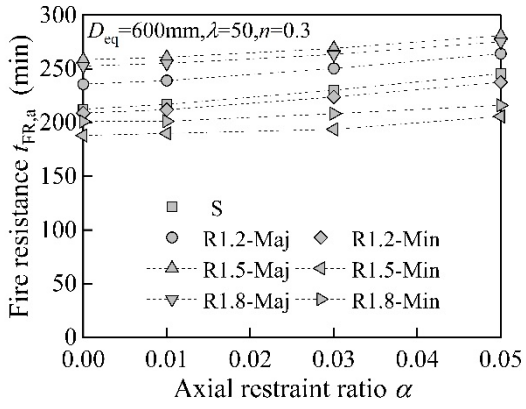

(e) D_{eq}=600mm, n=0.3, λ=50

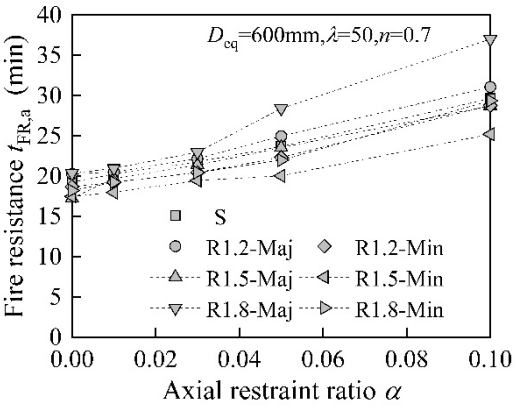

(f) D_{eq}=600mm, n=0.7, λ=50

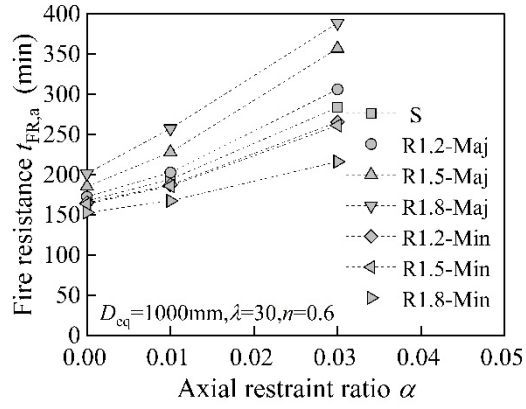

(g) D_{eq}=1000mm, n=0.6, λ=30

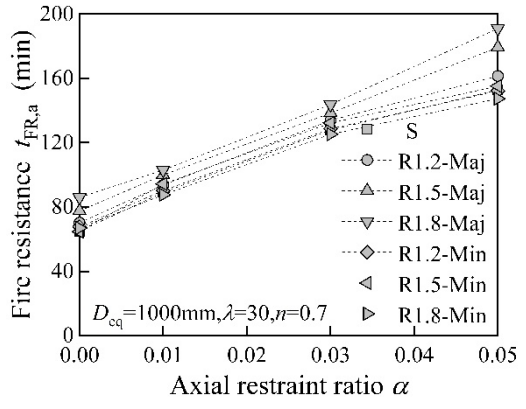

(h) D_{eq}=1000mm, n=0.7, λ=30

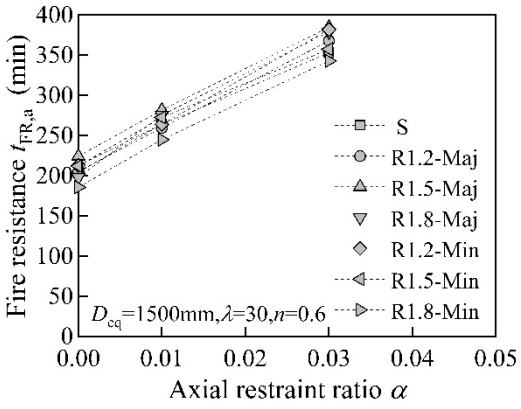

(i) D_{eq}=1500mm, n=0.6, λ=30

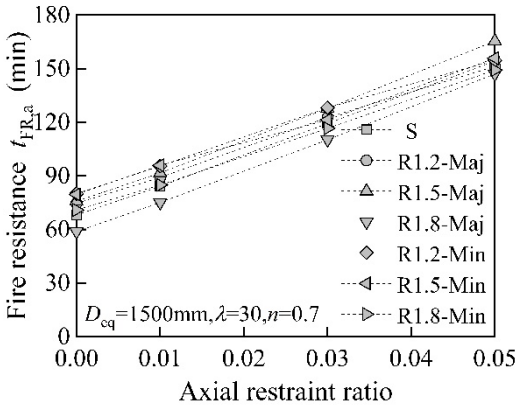

(j) D_{eq}=1500mm, n=0.7, λ=30

Fig. 8 Fire resistance of rectangular STRC columns subjected to various axial restraints

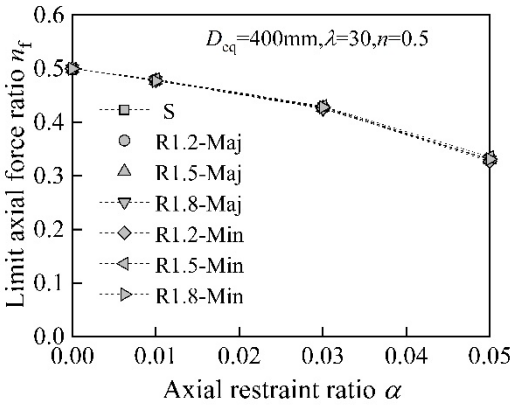

(a) D_{eq}=400mm, n=0.5, λ=30

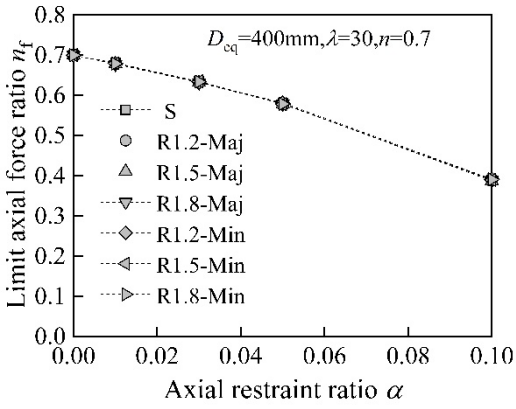

(b) D_{eq}=400mm, n=0.7, λ=30

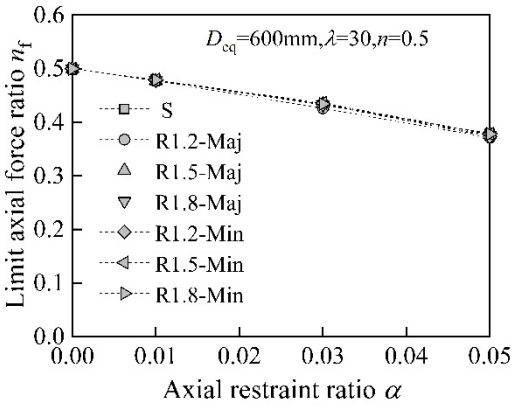

(c) D_{eq}=600mm, n=0.5, λ=30

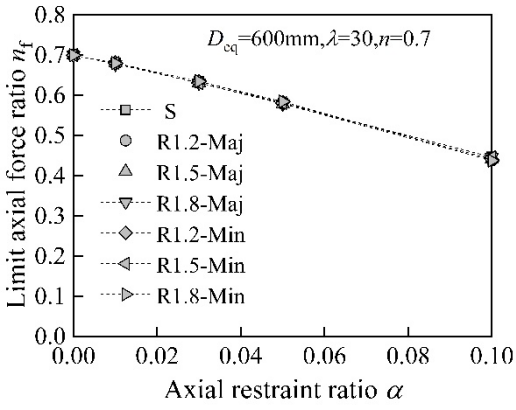

(d) D_{eq}=600mm, n=0.7, λ=30

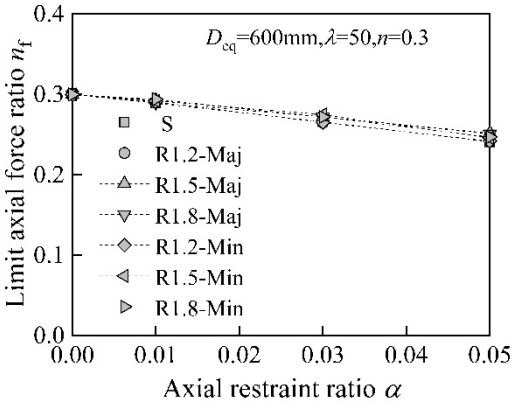

(e) D_{eq}=600mm, n=0.3, λ=50

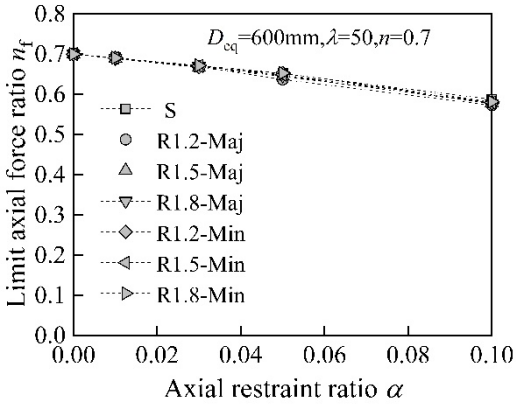

(f) D_{eq}=600mm, n=0.7, λ=50

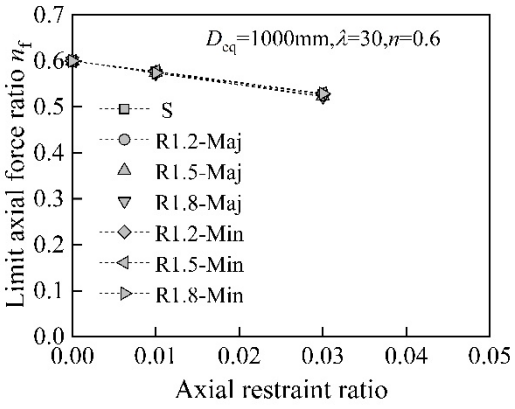

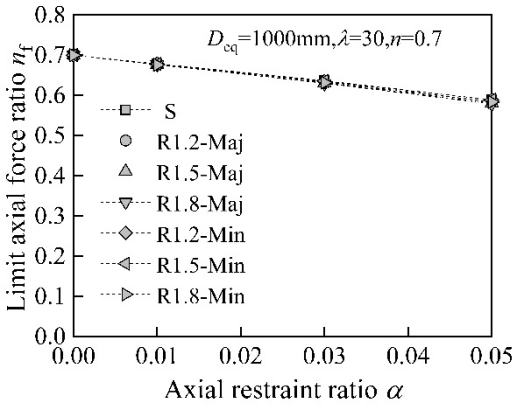

(g) D_{eq}=1000mm, n=0.6, λ=30

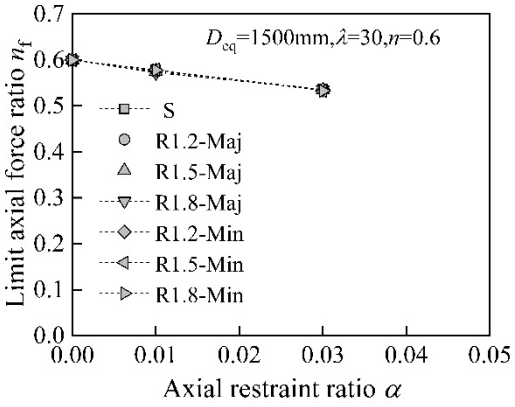

(h) D_{eq}=1000mm, n=0.7, λ=30

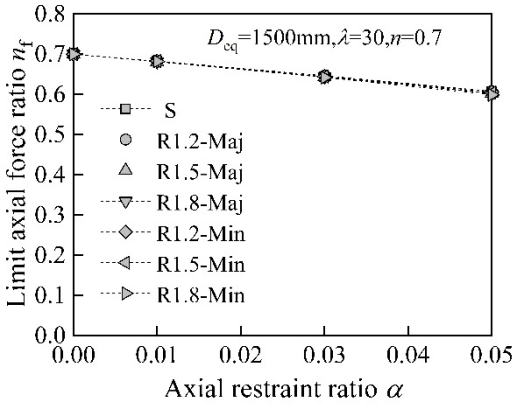

(i) D_{eq}=1500mm, n=0.6, λ=30

(j) D_{eq}=1500mm, n=0.7, λ=30

Fig. 9 Limit axial force ratios of rectangular STRC columns with different axial restraint ratios

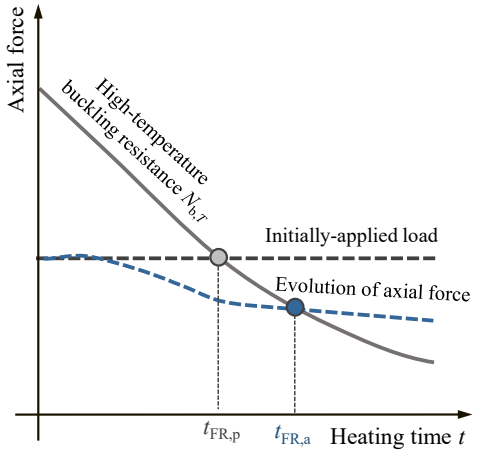

Fig.10 Illustration for the beneficial impact of axial restraint in enhancing the fire resistance of rectangular STRC columns

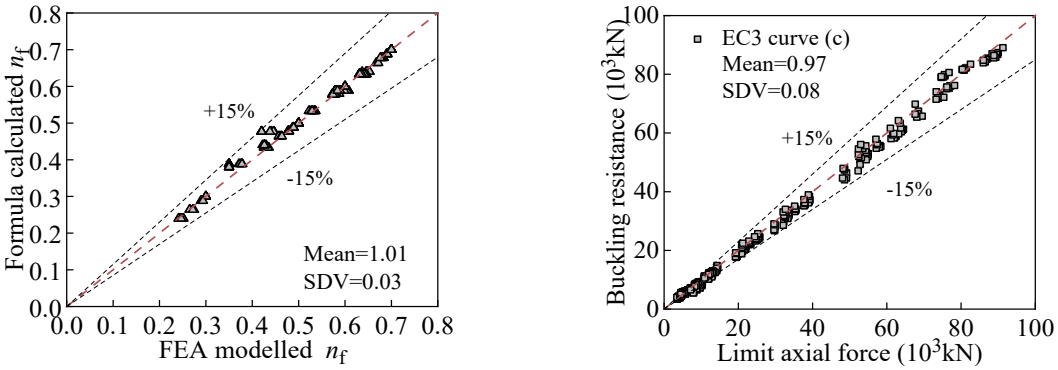

(a) Limit axial force ratio

(b) Buckling resistance

Fig. 11 Formula-calculated limit axial force ratio and buckling resistance compared to FEA results for rectangular STRC columns with axial restraints

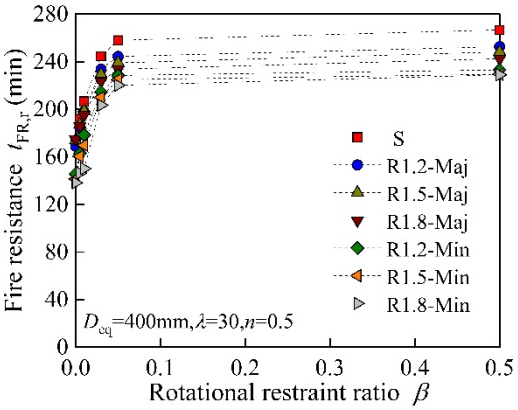

(a) D_{eq}=400mm, n=0.5, λ=30

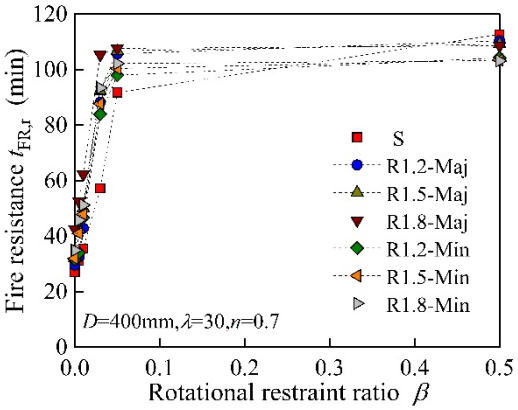

(b) D_{eq}=400mm, n=0.7, λ=30

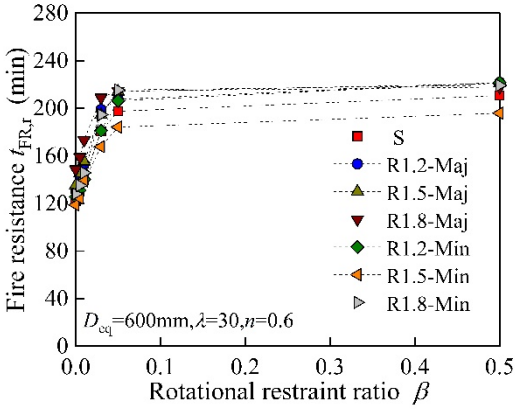

(c) D_{eq}=600mm, n=0.6, λ=30

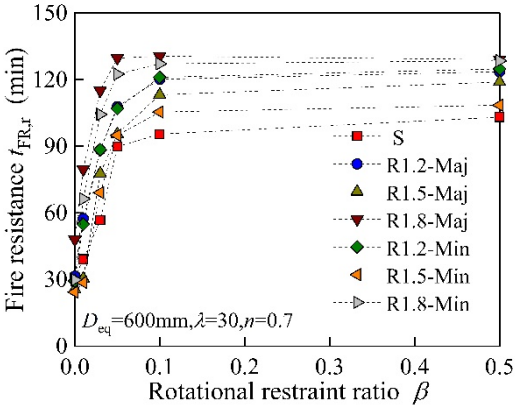

(d) D_{eq}=600mm, n=0.7, λ=30

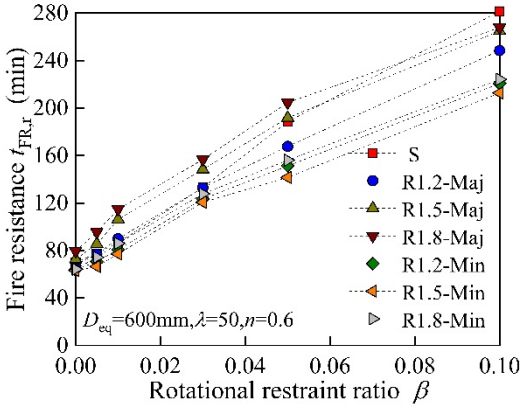

(e) D_{eq}=600mm, n=0.6, λ=50

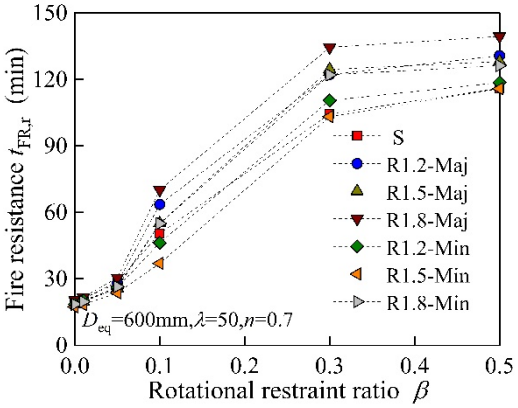

(f) D_{eq}=600mm, n=0.7, λ=50

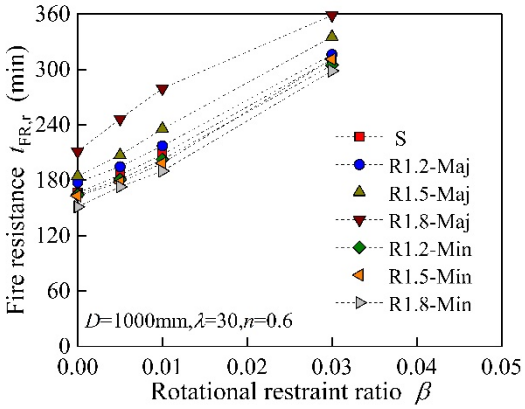

(g) D_{eq}=1000mm, n=0.6, λ=30

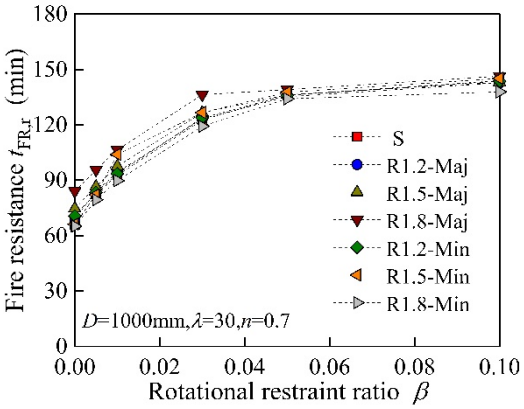

(h) D_{eq}=1000mm, n=0.7, λ=30

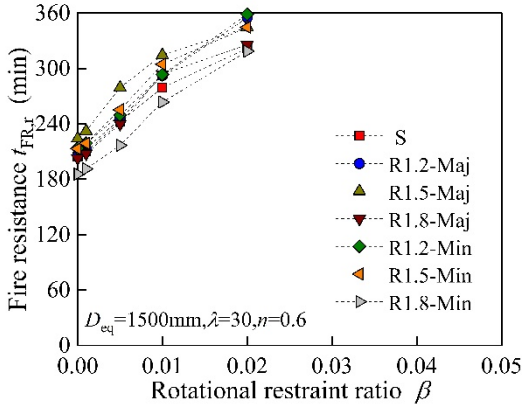

(i) D_{eq}=1500mm, n=0.6, λ=30

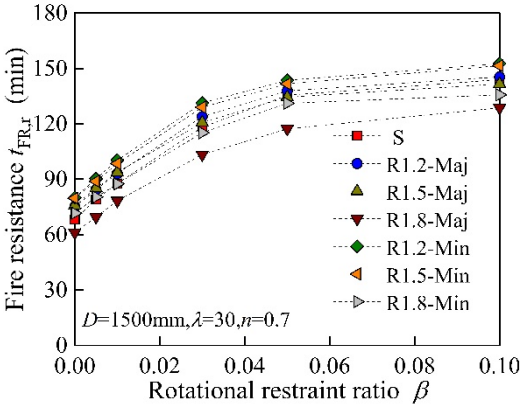

(j) D_{eq}=1500mm, n=0.7, λ=30

Fig. 12 Fire resistance of rotationally-restrained rectangular STRC columns

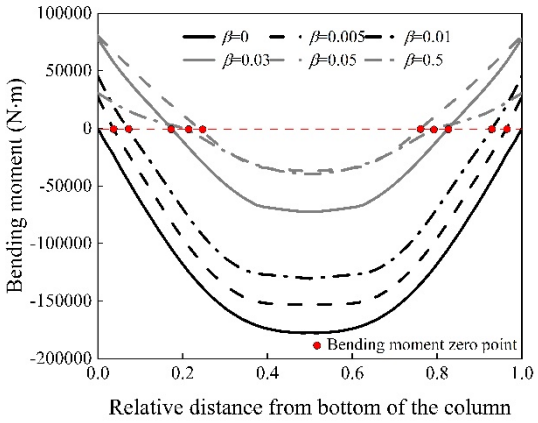

(a) R1.5-Maj (D_{eq}=600mm, λ=30, n=0.6)

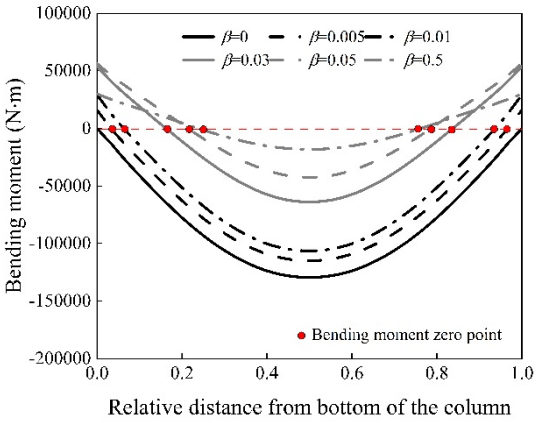

(b) R1.5-Min (D_{eq}=600mm, λ=30, n=0.6)

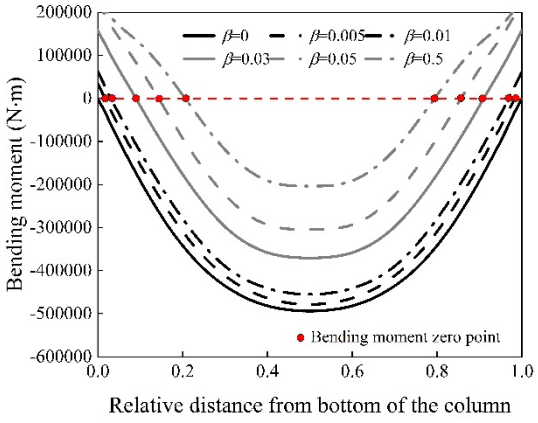

(c) R1.5-Maj (D_{eq}=600mm, λ=50, n=0.5)

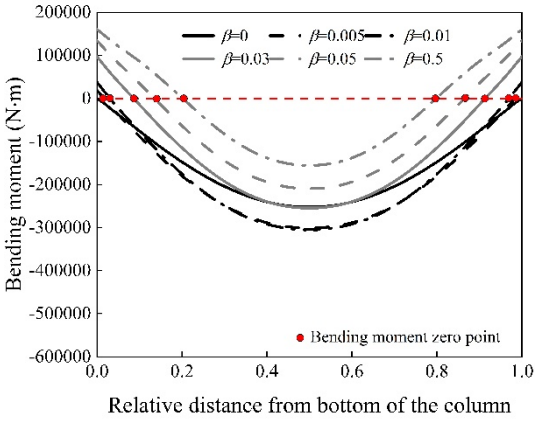

(d) R1.5-Min (D_{eq}=600mm, λ=50, n=0.5)

Fig. 13 Distributions of bending moments in rectangular STRC columns with rotational restraints at the failure state

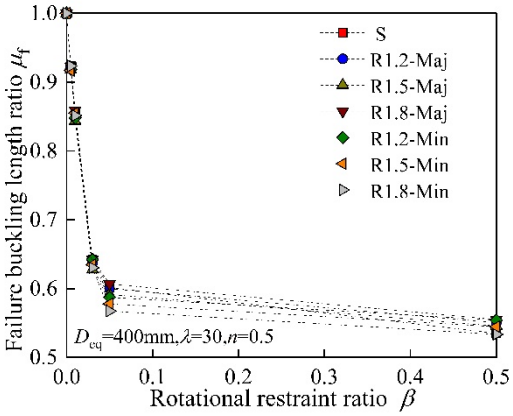

(a) D_{eq}=400mm, n=0.5, λ=30

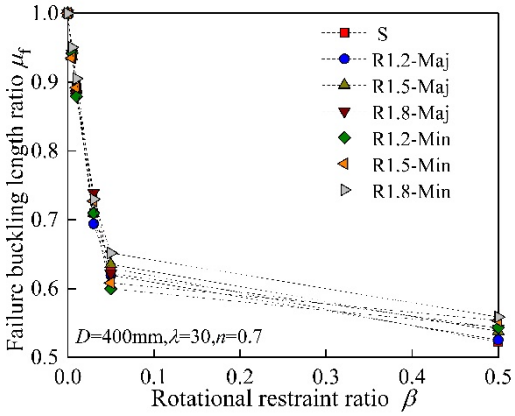

(b) D_{eq}=400mm, n=0.7, λ=30

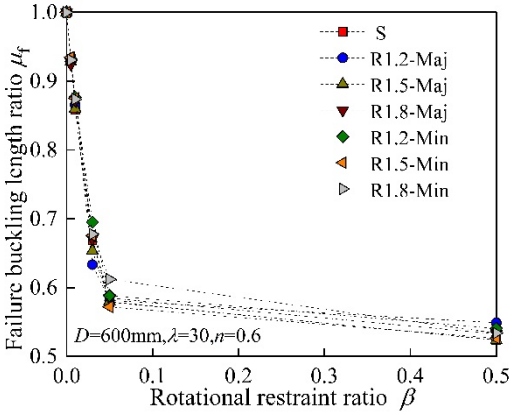

(c) D_{eq}=600mm, n=0.6, λ=30

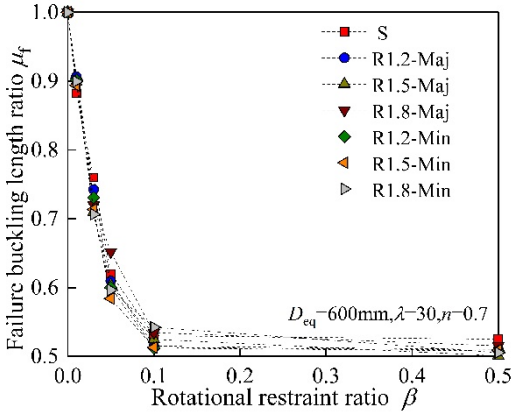

(d) D_{eq}=600mm, n=0.7, λ=30

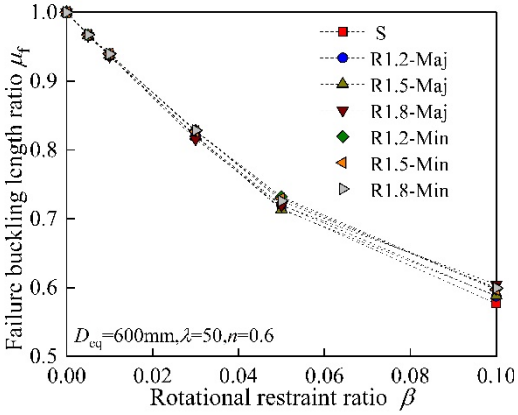

(e) D_{eq}=600mm, n=0.6, λ=50

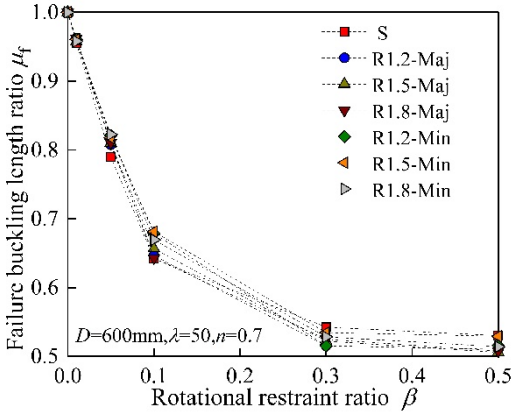

(f) D_{eq}=600mm, n=0.7, λ=50

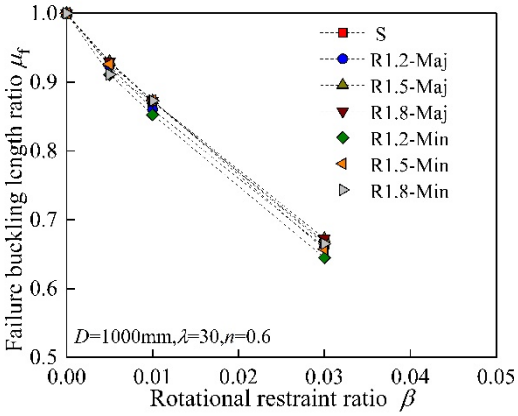

(g) D_{eq}=1000mm, n=0.6, λ=30

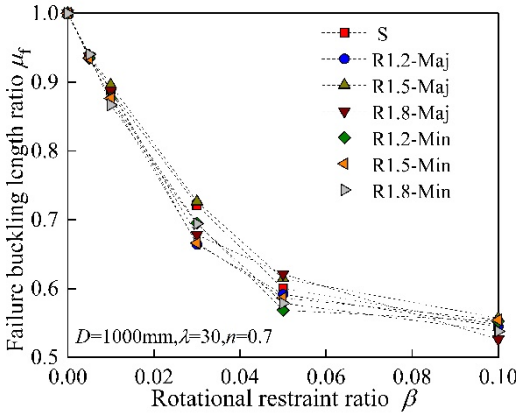

(h) D_{eq}=1000mm, n=0.7, λ=30

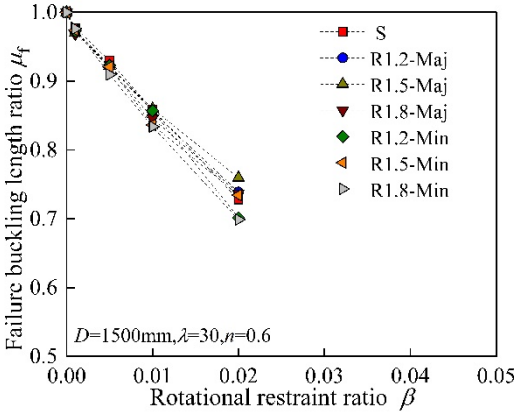

(i) D_{eq}=1500mm, n=0.6, λ=30

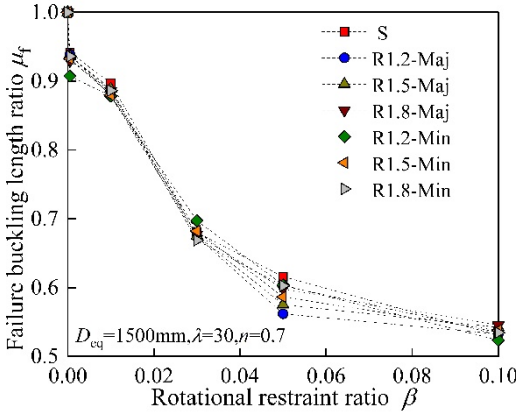

(j) D_{eq}=1500mm, n=0.7, λ=30

Fig. 14 Buckling length ratios of rotationally-restrained rectangular STRC columns

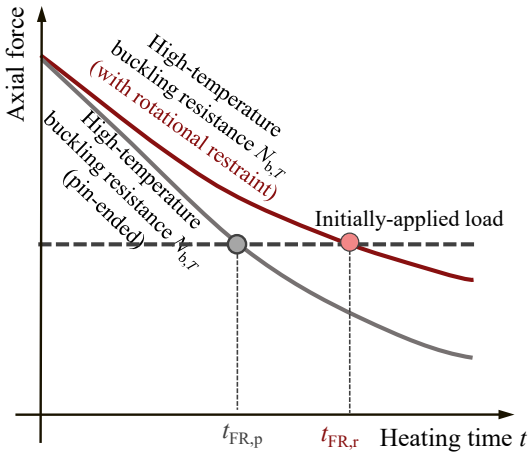

Fig. 15 Illustration for the advantageous impact of rotational restraint in improving the fire performance of rectangular STRC columns

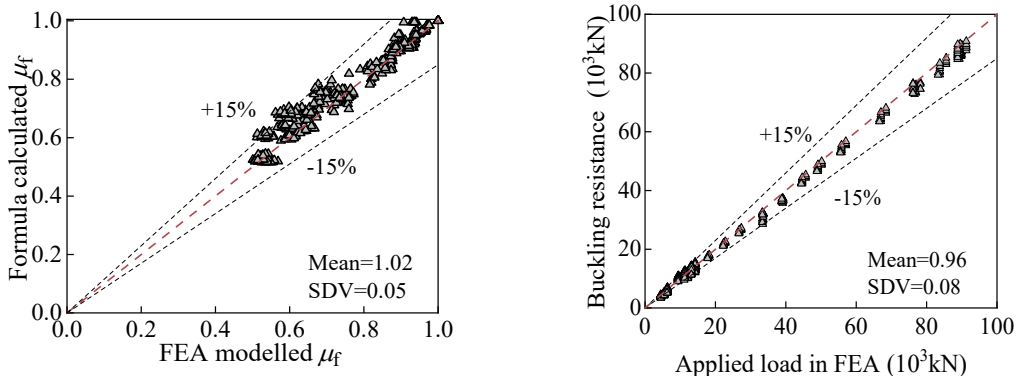

(a) Buckling length ratio (b) Buckling resistance

Fig.16 Formula-calculated failure buckling length ratio and buckling resistance compared to FEA results for rectangular STRC columns with rotational restraints

View publication stats